European Journal of Pharmacology 644 (2010) 138–145

Contents lists available at ScienceDirect

European Journal of Pharmacology

journal homepage: www.elsevier.com/locate/ejphar

Cardiovascular Pharmacology

Inhibitory effect of quercetin on matrix metalloproteinase 9 activity Molecular mechanism and structure–activity relationship of the flavonoid–enzyme interaction

Alejandra C. Saragusti [a,d], María G. Ortega [b,e], José L. Cabrera [b,e], Darío A. Estrin [c], Marcelo A. Marti [c,f,g,*], Gustavo A. Chiabrando [a,d,*]

[a] Centro de Investigaciones en Bioquímica Clínica e Inmunología (CIBICI), Consejo Nacional de Investigaciones Científicas y Técnicas (CONICET), Argentina
[b] Instituto Multidisciplinario de Biología Vegetal (IMBIV), Consejo Nacional de Investigaciones Científicas y Técnicas (CONICET), Argentina
[c] Instituto de Química-Física de Materiales, Medio Ambiente y Energía (INQUIMAE), Consejo Nacional de Investigaciones Científicas y Técnicas (CONICET), Argentina
[d] Departamento de Bioquímica Clínica, Universidad Nacional de Córdoba, Haya de la Torre y Medina Allende, Ciudad Universitaria (5000), Córdoba, Argentina
[e] Departamento de Farmacia, Facultad de Ciencias Químicas, Universidad Nacional de Córdoba, Haya de la Torre y Medina Allende, Ciudad Universitaria (5000), Córdoba, Argentina
[f] Departamento de Química Inorgánica, Analítica, y Química Física, Universidad de Buenos Aires, Ciudad Universitaria, Pabellón II, (C1428EHA) Ciudad de Buenos Aires, Argentina
[g] Departamento de Química Biológica, Facultad de Ciencias Exactas y Naturales, Universidad de Buenos Aires, Ciudad Universitaria, Pabellón II, (C1428EHA) Ciudad de Buenos Aires, Argentina

ARTICLE INFO

Article history:
Received 5 May 2010
Received in revised form 19 June 2010
Accepted 1 July 2010
Available online 7 July 2010

Keywords:
Diet polyphenol
Docking
Flavonoid
Molecular dynamics
Zymography

ABSTRACT

Epidemiological studies have demonstrated an inverse association between the consumption of flavonoid-rich diets and the risk of atherosclerosis. In addition, an increased activity of the matrix metalloproteinase 9 (MMP-9) has been implicated in the development and progression of atherosclerotic lesions. Even though the relationship between flavonoid chemical structure and the inhibitory property on MMP activity has been established, the molecular mechanisms of this inhibition are still unknown. Herein, we first evaluated the inhibitory effect of quercetin on MMP-9 activity by zymography and a fluorescent gelatin dequenching assay, secondly we determined the most probable sites and modes of quercetin interaction with the MMP-9 catalytic domain by using molecular modelling techniques, and finally, we investigated the structure–activity relationship of the inhibitory effect of flavonoids on MMP-9 activity. We show that quercetin inhibited MMP-9 activity with an IC_{50} value of 22 μM. By using docking and molecular dynamics simulations, it was shown that quercetin interacted in the S1′ subsite of the MMP-9 active site. Moreover, the structure–activity relationship analysis demonstrated that flavonoid $R^{3\prime}$–OH and $R^{4\prime}$–OH substitutions were relevant to the inhibitory property against MMP-9 activity. In conclusion, our data constitute the first evidence about the quercetin and MMP-9 interaction, suggesting a mechanism to explain the inhibitory effect of the flavonoid on the enzymatic activity of MMP-9, which provides an additional molecular target for the cardioprotective activity of quercetin.

1. Introduction

Matrix metalloproteinases (MMPs) are Zn^{II}-containing endopeptidases that share structural domains but differ regarding substrate specificity. The binding of peptide substrates to the active site occurs from left (N-terminus) to right (C-terminus), corresponding to the non-primed (S) and primed (S′) substrate binding subsites, respectively (Bode and Maskos, 2003). It is considered that the structural features most critical in determining the MMP substrate specificity, and thereby the inhibitor specificity, are contained within the zinc binding catalytic domain (Rao, 2005). MMPs, especially the gelatinase MMP-9, are involved in the remodelling of the extracellular matrix during the development and progression of atherosclerotic lesions (Newby, 2006). MMP-9 also plays an important role in the turnover of basement membrane type IV collagen during the formation of atherosclerotic plaques (Libby, 2002; Nguyen et al., 2001; Pasterkamp et al., 2000; Rahat et al., 2006; Stawowy et al., 2005).

Epidemiological studies in humans have shown an inverse association between the consumption of polyphenol-rich food and the risk of development and progression of atherosclerosis (Di Castelnuovo et al., 2002; Knekt et al., 1996; Mukamal et al., 2002; Peters et al., 2001). Among the polyphenols, quercetin is one of the most commonly found flavonoid in the human diet (Erlund et al., 2006). Several mechanisms by which quercetin may reduce the risk of atherosclerosis and cardiovascular disease have been proposed (Alcocer et al., 2002; Hayek et al., 1997; Osiecki, 2004; Pignatelli et al., 2000; Raso et al.,

* Corresponding authors. Chiabrando is to be contacted at CIBICI-CONICET, Haya de la Torre y Medina Allende, Ciudad Universitaria (5000) Córdoba, Argentina. Tel.: +54 351 4334164x103; fax: +54 351 4333048. Marti, INQUIMAE-CONICET, Ciudad Universitaria, Pabellón II, (C1428EHA) Ciudad de Buenos Aires, Argentina. Tel.: +54 11 45763378x124; fax: +54 11 45763341.
E-mail addresses: marcelo@qi.fcen.uba.ar (M.A. Marti), gustavo@fcq.unc.edu.ar (G.A. Chiabrando).

0014-2999/$ – see front matter © 2010 Elsevier B.V. All rights reserved.
doi:10.1016/j.ejphar.2010.07.001

2001; Welton et al., 1988), with one of these related to its ability to inhibit MMP-9 synthesis in vascular smooth muscle cells (Moon et al., 2003). In addition, it has been demonstrated that quercetin inhibits MMP gelatinase activity (MMP-9 and MMP-2), although only for relatively high concentrations (~100 μM) (Sartor et al., 2002). However, it was recently demonstrated that quercetin, and its major antioxidative quercetin metabolite quercetin-3-glucuronide (Q3GA), can accumulate, reaching micro-molar concentrations in atherosclerotic lesions (Kawai et al., 2008), which suggests that this flavonoid may be a potential inhibitor of MMP-9 activity at this site of inflammation. Nevertheless, even though the relationship between flavonoid chemical structure and the inhibitory property on MMP activity has been established, the molecular mechanisms of this inhibition are still unknown (Sartor et al., 2002). However, by using molecular modelling techniques, such as molecular docking and dynamics simulations, it may be possible to identify the putative interaction sites involved in the direct inhibition of active MMPs by flavonoids. In the present work, the main aim was to evaluate the inhibitory effect of quercetin on the MMP-9 activity by using a recombinant active form of this enzyme and a fluorescent gelatin dequenching assay. To investigate the most probable binding sites and modes of quercetin in the MMP-9 catalytic domain, both the above mentioned molecular modelling techniques and structure–activity relationship analysis were used.

2. Material and methods

2.1. Flavonoids and reagents

Quercetin (3,5,7,3′,4′-pentahydroxy-2-phenylchromen-4-one) was isolated and characterized following a procedure described previously (Guglielmone et al., 2002, 2005). Galangin (3,5,7-pentahydroxy-2-phenylchromen-4-one), quercetin-3-rutinoside (rutin), fisetin (3,7,3′,4′-pentahydroxy-2-phenylchromen-4-one), kaempferol (3,5,7,4′-pentahydroxy-2-phenylchromen-4-one), luteolin (5,7,3′,4′-pentahydroxy-2-phenylchromen-4-one), chrysin (5,7-pentahydroxy-2-phenylchromen-4-one) and epigallocatechin-3-gallate (EGCG) were purchased from Sigma (St. Louis, MO). The flavonoid general structure with the numbering pattern for rings A, B and C, and the different substitutions of the evaluated flavonoids are illustrated in Fig. 1. The stock solutions of flavonoids (1.0 mM) were prepared in 0.06% dimethyl sulfoxide (DMSO) in an enzyme buffer (50 mM Tris pH 7.4, containing 200 mM NaCl and 5 mM $CaCl_2$). The different concentrations of these compounds were obtained by diluting the stock solution in the enzyme buffer. In each case, fresh solutions were prepared and used immediately. Recombinant active MMP-9 was purchased from Calbiochem, Merk Biosciences, (Darmstadt, Germany); and DQ gelatin fluorescein conjugate was obtained from Molecular Probes (D-12054). All the reagents used were of analytical grade.

2.2. Assays for MMP-9 activity

2.2.1. Gelatin zymography

Aliquots of recombinant active MMP-9 (500 pg per lane) were assayed by gelatin zymography in 7.5% SDS-PAGE gel containing 0.15% (w/v) gelatin (Kleiner and Stetler-Stevenson, 1994). After electrophoresis, the gel was washed with 2.5% of Triton X100, cut into slides corresponding to MMP-9 bands, and incubated with different concentrations (25, 50, 75, 100 and 200 μM) of quercetin in the enzyme buffer used to develop the zymography. Gelatinolytic activity of MMP-9 was observed as clear bands against a blue-stained background, which were quantified by densitometric analysis using image software (UVP Vision Works® LS Image Acquisition and Analysis Software, Upland, CA). The data were expressed as the percentage of MMP-9 activity relative to control (without quercetin).

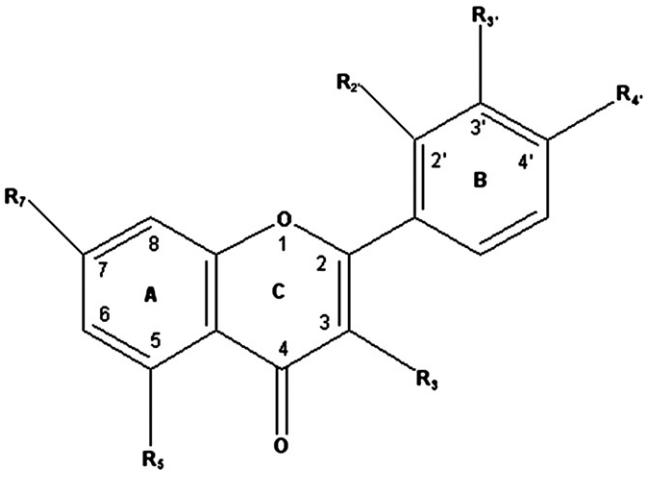

	3	5	7	2'	3'	4'
Quercetin	OH	OH	OH	H	OH	OH
Luteolin	H	OH	OH	H	OH	OH
Fisetin	OH	H	OH	H	OH	OH
Galangin	OH	OH	OH	H	H	H
Chrysin	H	OH	OH	H	H	H
Kaempferol	OH	OH	OH	H	H	OH
Morin	H	OH	OH	OH	H	OH

Fig. 1. Chemical structure of the evaluated flavonoids.

2.2.2. Fluorescent gelatin dequenching assay

Samples of recombinant active MMP-9 (250 ng/ml) were mixed with different concentrations (1, 10, 100 and 500 μM) of the evaluated flavonoids in enzyme buffer containing DQ gelatin (20 μg/ml) at 25 °C. Fluorescence was measured at $\lambda_{excitation} = 495$ nm and $\lambda_{emission} = 520$ nm using a standard fluorometer. The rates of hydrolysis were obtained from plots of fluorescence versus time (min), using data points from only the linear portion of the hydrolysis curve. Data were reported as the inhibition percentage of MMP-9 activity relative to the control (without flavonoid) as indicated in Eq. (1), where RC and RF correspond to the rate of hydrolysis for control and flavonoids, respectively.

$$\%Inhibition = [(RC - RF)/RC] \times 100 \quad (1)$$

The flavonoids for the concentrations studied did not interfere with fluorescent dequenching (results not shown). Values of IC_{50} (molar concentration of the compound that inhibits specific activity by 50%) were determined from the plot of % inhibition versus flavonoid concentration (μM) using non-linear regression analysis.

2.3. Docking and molecular dynamics simulations

2.3.1. Molecular structures and optimization

MMP-9 catalytic domain coordinates (without the fibronectin and prodomains) were obtained from the crystal structure (PDB ID: 1GKC) (Rowsell et al., 2002). The system consisted of one MMP-9 monomer, two catalytic and structural zinc ions, and three calcium ions. The zinc-ligand parameters were established following previous reports for docking and molecular dynamics simulations (Diaz and Suarez, 2007; Hu and Shelver, 2003). The staring structure for quercetin was built *in-silico* and subjected to a first full geometry optimization using AM-1. This initial optimization was followed by another full optimization using

the HF/631-G** combination method and basis set. Partial atomic charges were obtained from the corresponding optimized structures using the restrained electrostatic potential method (Wang et al., 2000), and all calculations were made with the Gaussian-98 package of programs (Frisch et al., 1998). The remaining non-bonded and internal parameters were simulated, using the generalized Amber force field for organic molecules (Wang et al., 2004).

2.3.2. Docking of quercetin in MMP-9 catalytic domain

Docking simulations were performed using the AutoDock 4.0 program package (Osterberg et al., 2002). Six structures of MMP-9 were selected (corresponding to the initial X-ray and 5 different snapshots from free MMP-9 molecular dynamics simulation) and subjected to ligand flexible docking simulations. For the first round of docking simulations a $100\times100\times100$ points grid with a 0.375 Å spacing, was built centered on the catalytic zinc ion, and then used to perform 100 independent runs. The results for each run were clustered together when the root mean square deviation between two putative structures of the inhibitor heavy atoms was less than 2.0 Å. Clusters were ranked based on their probability and their estimated binding energy (scoring). The grid box enclosed the entire MMP-9 substrate binding site and allowed complete rotation and translation of the ligand. The centers of mass of the highest probability and scoring clusters were selected for a second set of 100 docking runs, using a smaller and better resolved grid ($60\times60\times60$ points with a grid spacing of 0.25 Å). From these docking runs, plausible structures of flavonoid–MMP-9 complexes were selected for further molecular dynamics and thermodynamic analysis. The figures representing these quercetin–MMP-9 complex structures were made with VMD (Visual Molecular Dynamics) molecular graphics software (Humphrey et al., 1996) (http://www.ks.uiuc.edu/Research/vmd/).

2.3.3. Molecular dynamics simulations of quercetin–MMP-9 complexes and estimation of binding free energy

For all the molecular dynamics simulations, the starting structures, corresponding to free MMP-9 or flavonoid–MMP-9 complexes obtained from previous docking simulations, were immersed in a pre-equilibrated octahedral box of TIP3P water. Simulations were carried out at 1 atm and 300 K and maintained with the Berendsen barostat and thermostat, using periodic boundary conditions and Ewald sums (grid spacing of 1 Å) for treating long-range electrostatic interactions with a 10 Å cut-off (Berendsen et al., 1984). The SHAKE algorithm was used to keep bonds involving H (hydrogen) atoms at their equilibrium length (Ryckaert et al., 1977), and a 2 fs time step was used for the integration of Newton's equations. The Amber ff99SB force field parameters were used for all protein residues (Hornak et al., 2006), with all simulations being performed with the particle mesh Ewald molecular dynamics module of the AMBER9 program (Hornak et al., 2006; Pearlman et al., 1995). The equilibration protocols consisted of performing an optimization of the initial structures, followed by a slow heating up to the desired temperature. This heating was performed in 200 ps of constant volume molecular dynamics, followed by 200 ps of simulation at constant pressure. Once the system was equilibrated, the different production runs were performed. The quercetin–MMP-9 complex structures selected after docking were subjected to 5 ns long simulations in explicit solvent, using the parameters mentioned above. From these simulations, a computationally efficient molecular mechanics approach was used coupled to a continuum representation of solvent effects called the molecular mechanics Poisson–Boltzmann surface area (Lee et al., 2000). The binding free energy (ΔG_B) as well as its contributions were computed for each structure using Eq. (2), where ΔE_{GAS} corresponds to the ligand binding energy in the gas phase (i.e. in vacuum), and ΔE_{ELEC} and ΔE_{VDW} are the corresponding electrostatic and van der Waals contributions to the energy, respectively.

$$\Delta E_{GAS} = \Delta E_{ELEC} + \Delta E_{VDW} \tag{2}$$

In addition, the solvation free energy (ΔG_{SV}) contribution to the binding was estimated using the Poisson–Boltzmann implicit solvation method (Lu and Luo, 2003). Then, adding ΔE_{GAS} and ΔG_{SV} as indicated in Eq. (3) permitted ΔG_B to be estimated.

$$\Delta G_B = \Delta G_{SV} + \Delta E_{GAS} \tag{3}$$

Given the inherent difficulties in computing the solvation free energies, the ΔG_{SV} values should be analyzed carefully and considered together with the more robust ΔE_{GAS} contribution. Hydrogen bond interactions between quercetin and MMP-9 were classified as weak or strong bonds, based on the analysis of their structural fluctuations along the molecular dynamics simulation. Strong bonds remained formed for more than 95% of the simulation time, while weak hydrogen bonds were those that broke and formed again during the dynamics.

2.4. Statistical analysis

Results were expressed as the mean ± S.E.M. of independent experiments. A one-way ANOVA was used for comparisons. Differences from the control with $P<0.05$ were considered significant.

3. Results

3.1. Inhibitory effect of quercetin on MMP-9 activity

Previously it was reported that quercetin exerts a weak inhibition on MMP-9 activity for inhibitory concentrations higher than 100 μM (Sartor et al., 2002). These authors determined the MMP-9 activity by gelatin zymography, using latent MMP-9 (pro-MMP-9 activated by 4-aminophenylmercuric acetate) obtained from the cell culture-conditioned medium of HT-1080 human fibrosarcoma cells. In our work, a pure and recombinant active MMP-9 was used, and the enzyme activity was determined by gelatin zymography and a fluorescent gelatin dequenching assay. In this way, we evaluated different concentrations of quercetin (1 to 500 μM) for constant amounts of active MMP-9. Fig. 2 shows a representative zymography analysis, where it can be observed that quercetin produced in a concentration-dependent manner a significant decrease in the MMP-9 activity. Densitometric analysis showed that quercetin concentrations between 25 μM and 100 μM produced a significant inhibition on the MMP-9 activity. In addition, in order to obtain quantitative inhibitory data related to this, a fluorescent dequenching assay was used. By considering standardized kinetic parameters for this assay (Supplementary Fig. 1) we determined that quercetin inhibited the MMP-9 activity in a concentration-dependent manner, resulting in an IC_{50} value of 22 μM (Fig. 3). Thus, these data indicate that quercetin inhibited the MMP-9 activity for inhibitory concentrations lower than 100 μM.

3.2. Theoretical evaluation of the most probable sites and modes of the quercetin interaction in the MMP-9 catalytic domain

To investigate the molecular basis of the inhibitory effect of quercetin on the MMP-9 activity, we evaluated the putative sites and modes of quercetin interaction in the MMP-9 catalytic domain by combining docking and molecular dynamics simulations. The docking analysis of quercetin in the MMP-9 catalytic domain showed that the highest probability and scoring clusters displayed docking binding energies between −5.0 and −7.0 kcal mol^{-1}, which were located at different

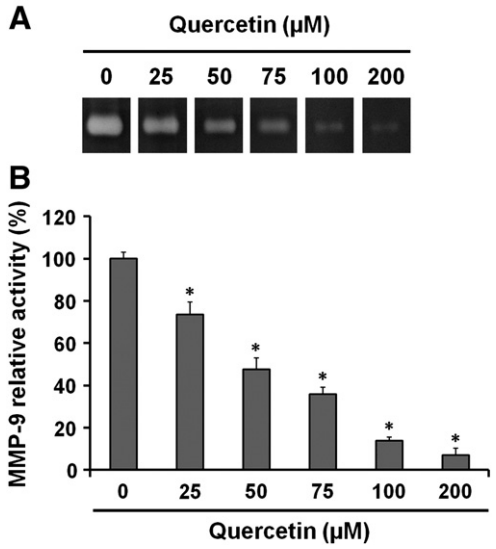

Fig. 2. Zymography analysis of MMP-9 activity incubated with different concentrations of quercetin. A) Representative zymography assays of MMP-9 gelatinolytic activity. B) Densitometry analysis from zymography assays. The bars represent the results expressed as a percentage of the MMP-9 activity in the absence of quercetin. The standard errors of the mean obtained from triplicate experiments are indicated, with the asterisk (*) denoting *P* values (<0.05) significantly different to control (0 μM of quercetin).

substrate binding subsites in the active site cleft. The most stable docking structures were then selected, and from each binding mode the interaction was optimized by molecular dynamics simulation. The two most favourable binding modes of quercetin with the MMP-9 catalytic domain were obtained (Table 1), based on the lowest ΔG_B values, which were at least two fold smaller than those of the other possible interaction modes. Complexes 1 and 2 showed quite similar ΔG_B, ΔE_{GAS} and ΔG_{SV}, and located quercetin at the active site S′ subsite. The main difference between both complexes was related to the energy values corresponding to ΔE_{ELEC} and ΔE_{VDW} (Table 1). Fig. 4 shows the interaction site and mode of quercetin in complex 1, where the benzene (ring B) was located inside the hydrophobic cavity of the S′ subsite, whereas its chromone (ring A and ring C) pointed towards the S2′ subsite (Fig. 4A and B). Also, Fig. 4C reveals that the quercetin benzene was held inside the S1′ pocket, bounded by the catalytic zinc-ligand His^{401} (on the left), the backbone residues 421 to 424 of the specificity loop (at the front), and the active site helix B (at the back). A strong hydrogen bond interaction was established between the Met^{422} of the S1′ wall-forming segment and the R$^{3\prime}$–OH, whereas a weak hydrogen

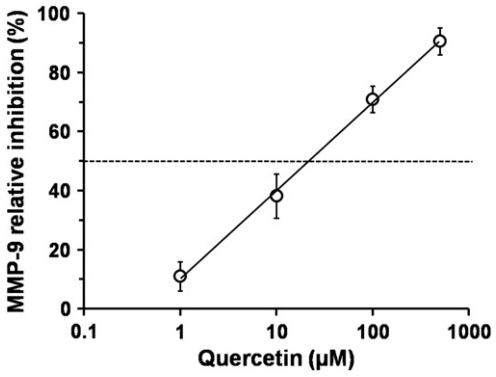

Fig. 3. Concentration-dependent inhibitory analysis of quercetin on the MMP-9 activity determined by a fluorescent gelatin dequenching assay. The results are expressed as a percentage of inhibition of the MMP-9 activity obtained in the absence of quercetin. The standard errors of the mean obtained from triplicate experiments are indicated. The dotted line indicates a 50% inhibition of MMP-9 activity, which represents an IC_{50} value of 22 μM of quercetin.

Table 1
Binding subsites and binding free energies wit their contributions for the mostfavorable quercetin-MMP-9 complex structures (1 and 2).

Complex Structure	Binding Subsites	ΔG_B[a]	ΔE_{GAS}[b]	ΔG_{SV}[c]	ΔE_{ELEC}[d]	ΔE_{VDW}[e]
1	S1′,S2′	−15.9	−60.3	−44.4	−17.1	−43.2
2	S2′,S3′	−14.8	−56.9	−42.1	−28.5	−28.4

bond existed between Ala^{417} of the "met-turn" and the R$^{4\prime}$–OH. With respect to the quercetin chromone, Fig. 4C shows that it was partially shielded from the solvent by the backbone of residues 186 to 190. The hydrophobic interactions were established between the chromone and the side chain of Leu^{188} and Val^{398}, and two strong hydrogen bonds existed between the quercetin R^5–OH with the Leu^{188} and Ala^{189} of the edge strand of β-strand IV. In addition, for this complex, the quercetin

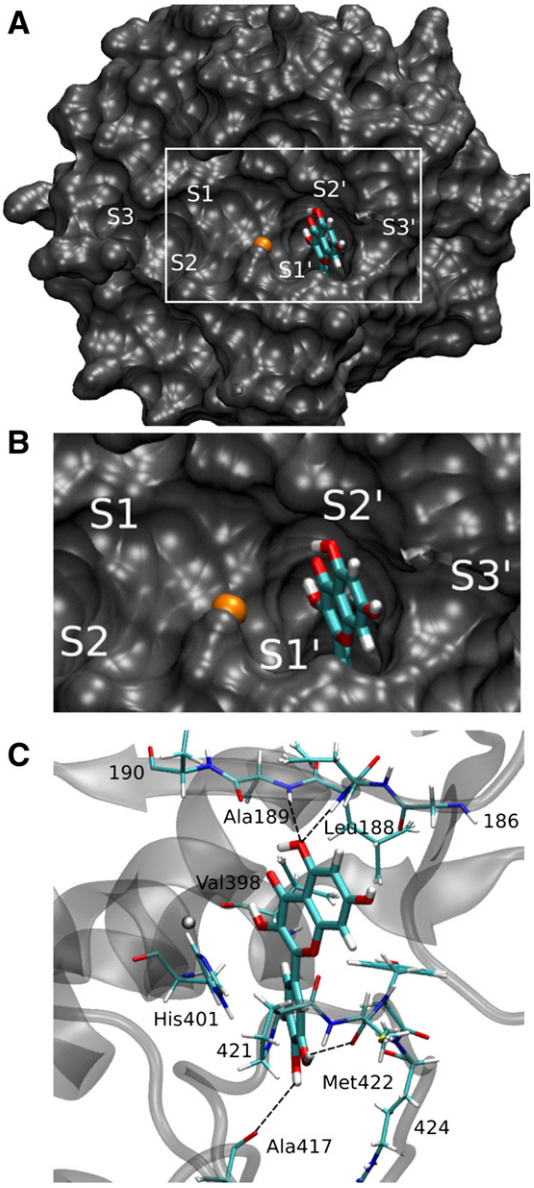

Fig. 4. Quercetin MMP-9 complex structure 1. A) The MMP-9 structure is shown as a gray vdw surface and quercetin appears as sticks. The catalytic zinc ion is shown as an orange sphere, and the S and S' binding sites are labeled in white. B) A close up of a). C) Close up of the quercetin MMP-9 hydrogen bond (black dashed lines) interactions.

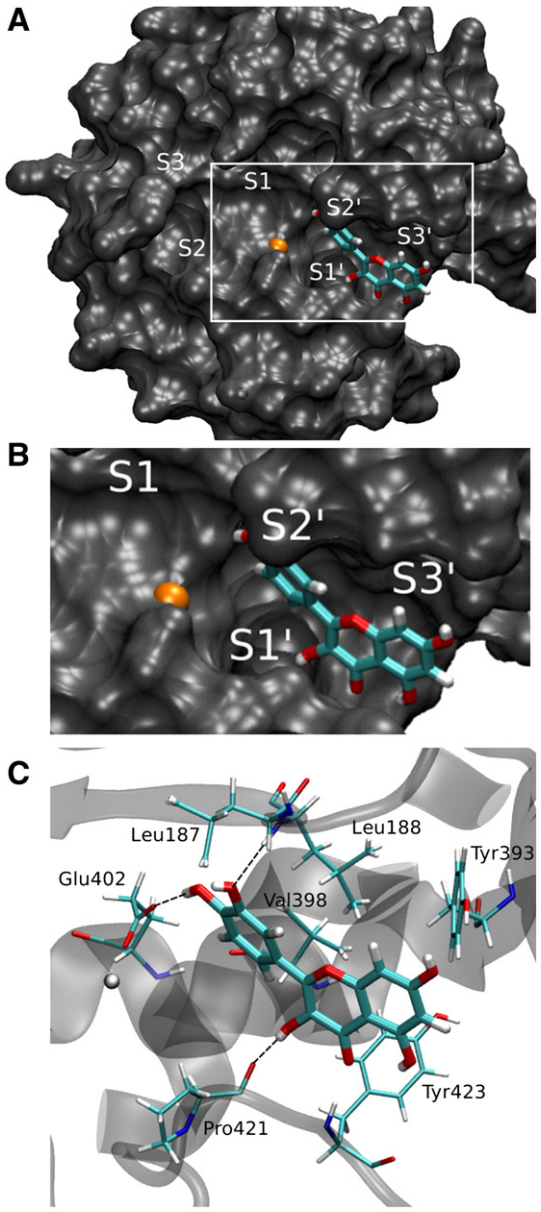

Fig. 5. Quercetin–MMP-9 complex structure 2. A) The MMP-9 structure is shown as a gray vdw surface and quercetin appears as sticks. The catalytic zinc ion is shown as an orange sphere, and the S and S' binding sites are labeled in white. B) A close up of a). C) Close up of the quercetin–MMP-9 hydrogen bond (black dashed lines) interactions.

oxygens were located at a distance of more than 5 Å from the catalytic zinc ion, which implies that the interaction between the flavonoid and the enzyme involved no chelation. Fig. 5 shows the interaction site and mode of quercetin in complex 2. The quercetin benzene was placed towards S2′ and its chromone located at the S3′ subsite of the enzyme, with these subsites being more exposed to solvant than S1′ (Fig. 5A and B). The hydrophobic interactions occurred between the benzene and the residues Leu^{187} and Leu^{188} (S2′ subsite), and Val^{398} (back side of S1′). In addition, the quercetin chromone ring was located at the edge of the MMP-9 active site interacting with Tyr^{393} (S3′) and Tyr^{423} (S1′). Two strong hydrogen bonds were formed for $R^{4\prime}$–OH with active site Glu^{402} and the $R^{3\prime}$–OH and Leu^{188}–NH, and a weak hydrogen bond existed between R^3–OH and the carbonyl of Pro^{421} of the wall-forming segment. In this complex, quercetin oxygens were not capable of zinc-coordination.

3.3. Structure–activity relationship

Considering the structural data obtained from the docking and molecular dynamics analysis of the quercetin–MMP-9 complexes 1 and 2, we hypothesize that the inhibitory effect of quercetin on the MMP-9 activity involved interaction between the MMP-9 residues and the quercetin hydroxyl substitutions, at $R^{3\prime}$ and $R^{4\prime}$ of the B ring (complexes 1 and 2), R^5 (complex 1) and R^3 (complex 2) of the chromone. For this reason, we investigated the structure–activity relationship of the inhibitory effect of flavonoids on MMP-9 activity, by using flavonoids that contained the different hydroxyl substitutions represented in Fig. 1, with the inhibitory properties of these compounds on the MMP-9 activity being determined by a fluorescent gelatin dequenching assay. When luteolin and fisetin were assayed, compounds having both $R^{3\prime}$ and $R^{4\prime}$ hydroxyl substitutions, they showed an inhibitory effect comparable to quercetin at a flavonoid concentration of 100 μM (Fig. 6A). On the other hand, assays of galangin and chrysin, compounds lacking these $R^{3\prime}$ and $R^{4\prime}$ hydroxyl substitutions, did not result in a significant inhibitory effect on the MMP-9 activity at 100 μM (Fig. 6A). These results demonstrate that the presence of the hydroxyl substitutions at $R^{3\prime}$ and $R^{4\prime}$ of the quercetin B ring constitutes a relevant structural feature in the MMP-9 activity inhibition. However, the structure–activity relationship analysis data indicate that the presence of two hydroxyl substitutions at R^3 and R^5 together did not contribute to the inhibitory ability of quercetin, since luteolin and fisetin (which conserved only one of these hydroxyl substitutions) had a similar MMP-9 inhibitory effect to that of quercetin (Fig. 6A).

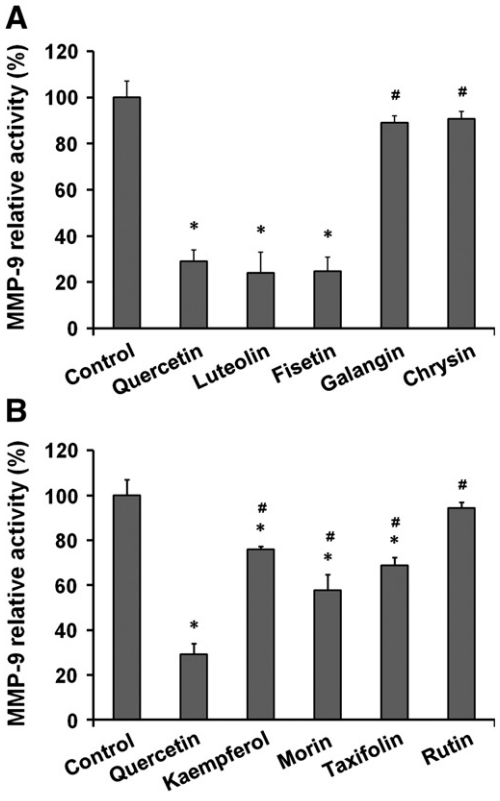

Fig. 6. Flavonoid effect on MMP-9 activity for a 100 μM concentration of the compounds. The bars represent the results obtained by a fluorescent gelatin dequenching assay expressed as a percentage of MMP-9 activity in the absence of compounds. The standard errors of the mean obtained from triplicate experiments are indicated. The quercetin effect compared with: A) luteolin, fisetin, galangin and chrysin; and B) kaempferol, morin, taxifolin and rutin. The asterisk (*) denotes *P* values (<0.05) significantly different to control (0 μM of compounds). The symbol (#) denotes *P* values (<0.05) significantly different to quercetin.

Taking into consideration that $R^{3\prime}$ and $R^{4\prime}$ hydroxyl substitutions were involved in the inhibitory effect of quercetin on the MMP-9 activity, we now evaluated compounds with different hydroxyl patterns in the B ring. Kaempferol and morin showed a lower inhibitory effect with respect to quercetin at 100 μM (Fig. 6B), with these data strongly suggesting that the presence of the two hydroxyl substitutions (at $R^{3\prime}$ and $R^{4\prime}$), situated ortho to each other in the structure, potentiated the inhibitory ability on the MMP-9 activity. In addition to the hydroxilation profile, another structural feature that may have favoured the interaction between quercetin and MMP-9 is the 2,3-double bond of the flavonoid C ring, which confers a planar structure. As shown in Fig. 6B, taxifolin, which lacks the 2,3-double bond, showed a lower inhibitory effect on MMP-9 activity than quercetin at 100 μM, demonstrating that the planarity of the molecule contributed favourably to the quercetin–MMP-9 interaction. Finally, the effect of quercetin *o*-glycosylation at R^3 was evaluated by testing rutin on the MMP-9 activity, with Fig. 6B demonstrating that the sugar moiety eliminated the inhibitory capacity of quercetin.

Based on the structure–activity relationship analysis indicated above, we determined the concentration-dependent inhibitory effect of the flavonoids on the MMP-9 activity and calculated the IC_{50} values. EGCG was used as a control for the enzyme inhibition, since this flavonoid is considered to be a potent MMP-9 inhibitor (Demeule et al., 2000). Fig. 7 shows the inhibitory analysis for different concentrations of flavonoids, ranging from 1×10^{-6} to 0.5×10^{-3} M. The control EGCG showed an important inhibitory effect on MMP-9 activity with an IC_{50} value of 0.2 μM, (Fig. 7), comparable with the previously informed value of 0.3 μM using an EnzChek Gelatinase kit with the same substrate and source of MMP-9 (Demeule et al., 2000). Three distinct groups of compounds were observed, based on their inhibitory capacity against MMP-9 activity. In the first group, quercetin, luteolin and fisetin were the most potent inhibitors with IC_{50} values of 22, 8, and 6 μM, respectively. The second group was made up of weaker MMP-9 inhibitors: kaempferol, morin and taxifolin, which had IC_{50} values of 500, 142, and 364 μM, respectively. Finally, the last group included compounds that had extremely poor inhibitory effects on MMP-9 activity, namely, galangin, chrysin and rutin. These all had estimated IC_{50} values higher than 500 μM.

4. Discussion

In this study, we have investigated the inhibitory effect of flavonoids, in particular quercetin, on the enzymatic activity of active MMP-9. Previously, only one report has examined the inhibitory property of different flavonoids on MMP activity, where a weak inhibitory effect of quercetin was established for concentrations higher than 125 μM (Sartor et al., 2002). However, herein we demonstrate that quercetin significantly inhibited the MMP-9 activity at lower concentrations than those previously reported. These discrepant results could be due to different conditions occurring in the gelatinolytic assays used to evaluate the inhibitory effect of quercetin, which may be mainly attributed to the source of the active MMP-9 as well as to the optimal molar ratios of quercetin/MMP-9 used for the inhibitory assay. In the present work, in order to optimize the experimental conditions, a recombinant active MMP-9 form was used, with two different gelatinolytic techniques, zymography and fluorescent gelatin dequenching assay, being standardized. By using both these methods, we determined that quercetin concentrations lower than 100 μM produced a significant inhibition of MMP-9 activity (Fig. 2), with an IC_{50} value of 22 μM (Fig. 3). Thus, our data clearly indicate that quercetin inhibited the enzymatic activity of MMP-9.

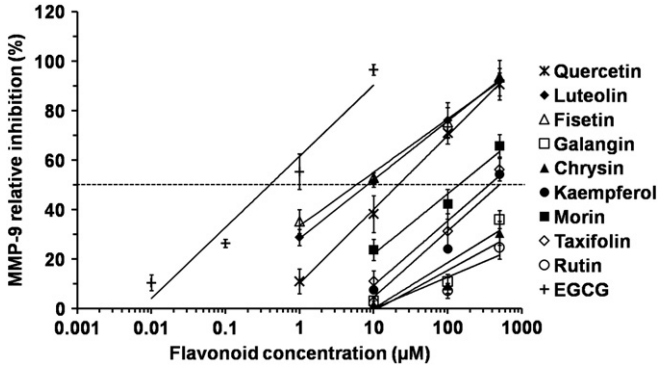

Fig. 7. Concentration-dependent inhibitory analysis of flavonoids on the MMP-9 activity determined by a fluorescent gelatin dequenching assay. The results are expressed as a percentage of inhibition of the MMP-9 activity obtained in the absence of the compounds. The standard errors of the mean obtained from triplicate experiments are indicated. The dotted line indicates a 50% inhibition of MMP-9 activity, which represents an IC_{50} values of 0.2 μM (EGCG); 6 μM (fisetin); 8 μM (luteolin); 22 μM (quercetin); 142 μM (morin); 364 μM (taxifolin); 500 μM (kaempferol); and >500 μM (galangin, chrysin and rutin).

The determination of inhibitor–enzyme complex structures with atomic detail is necessary for understanding the molecular basis of the inhibitor function. Several three-dimensional structures of MMPs in complexes with synthetic inhibitors have been determined by X-ray crystallography and molecular modelling methods (Bertini et al., 2007; Diaz and Suarez, 2007; Hu and Shelver, 2003; Lang et al., 2001; Pavlovsky et al., 1999; Rowsell et al., 2002; Tuccinardi et al., 2006). In contrast, only a few three-dimensional structures of flavonoids in complexes with mammalian enzymes (for instance PI3-K, elastase and uPA) have been solved (Cuccioloni et al., 2009; Walker et al., 2000). In addition, although the complex structures of flavonoids with MMPs have not been previously reported either by crystallography or molecular modelling techniques, in the present work, by using docking and molecular dynamics simulations, it was shown that quercetin formed two stable complex structures (complexes 1 and 2) with MMP-9 catalytic domain. Furthermore, in both these structures, quercetin was observed to interact in the S1′ subsite of the MMP-9 active site, and interestingly, the majority of the reported synthetic MMP inhibitors were shown to bind into this substrate subsite (Cuniasse et al., 2005; Kiyama et al., 1999; Li and Xu, 2004; Rao, 2005), considered to be the most important in terms of substrate and inhibitor specificity (Bode et al., 1999; Pirard and Matter, 2006).

It has been proposed that both the number and localization of hydroxyl substitutions determine the biological activity of flavonoids. In this sense, R^3–OH has been reported to be strongly related to the antioxidant capacity in the majority of flavonols (Silva et al., 2002). Another structural feature relevant for the biological effect is the orto-diphenolic arrangement in the B ring (Matsuda et al., 2002; Rice-Evans et al., 1996). In addition to the hydroxyl substitutions, the 2,3-double bond in the C ring and the 4-oxo group may also influence flavonoid activity (Rice-Evans et al., 1996; Zhang et al., 2005). In the present work, by using docking and molecular dynamics analysis, we demonstrated that the number and localization of hydroxyl substitutions in quercetin influence its interaction with the MMP-9 catalytic domain. In complex 1, the quercetin hydroxyls involved in the hydrogen bond interaction with the MMP-9 catalytic domain were $R^{3\prime}$–OH and $R^{4\prime}$–OH of the B ring, and R^5–OH from the chromone ring (Fig. 4). In complex 2, $R^{3\prime}$–OH and $R^{4\prime}$–OH were also implicated in hydrogen bond interaction, but R^3–OH instead of R^5–OH was the hydroxyl substituent from the chromone ring that stabilized the structure (Fig. 5). Moreover, by using structure–activity relationship analysis with structurally different flavonoids, we further demonstrated the relevance of $R^{3\prime}$–OH and $R^{4\prime}$–OH, since luteolin and fisetin showed a similar inhibitory action on MMP-9 activity as quercetin at a 100 μM concentration (Fig. 6A). In addition, these compounds had similar IC_{50} values to that of quercetin (Fig. 7), which supports the possibility that at least one of these substitutions (R^3–OH or R^5–OH) is probably needed to stabilize the flavonoid in the active site of MMP-9. The relevance of $R^{3\prime}$–OH and $R^{4\prime}$–OH substitutions of the B ring on the

inhibitory property against MMP-9 activity was also demonstrated in flavonoids lacking these hydroxyls in the flavonoid structure. Neither galangin nor chrysin showed any significant inhibitory effect on MMP-9 activity, in comparison to quercetin, fisetin and luteolin (Figs. 6A and 7). Thus, we conclude that $R^{3\prime}$–OH and $R^{4\prime}$–OH substitutions in flavonoids are relevant to the inhibitory property on the enzymatic activity of active MMP-9.

Further analysis of the involvement of the hydroxylation pattern of B ring in the inhibitory capacity of MMP-9 activity showed that the presence of two hydroxyl substitutions at the ortho position potentiated the inhibitory effect, since kaempferol (containing only the $R^{4\prime}$–OH substitution) and morin (having a meta-diphenolic arrangement) had less inhibitory potency than quercetin, fisetin or luteolin (Figs. 6B and 7). Moreover, the 2,3-double bond in the C ring was also relevant for this inhibitory property, since taxifolin, which differs from quercetin with respect to this structural feature, showed a poor inhibitory effect on MMP-9 activity (Figs. 6B and 7). Finally, the absence of an inhibitory effect of rutin (Figs. 6B and 7) could have been due to the rutinoside moiety at C3, which affects the ability of the hydroxyl substitutions to reach and interact with the subsites of the MMP-9 catalytic domain.

An important number of *in vivo* and epidemiological studies have demonstrated that flavonoids exert many biological effects with relevant cardioprotective action (Huxley and Neil, 2003; Maron, 2004; Middleton et al., 2000; van't Veer et al., 2000). Related to this, an inverse association has been reported between the consumption of flavonoid-rich diets and the risk of atherosclerosis (Brambilla et al., 2008; Giovannini et al., 2007). However, the molecular mechanisms implicated in the beneficial actions of these natural compounds in human health are diverse and complex. Several *in vitro* assays have reported that flavonoids inhibit the mammalian enzyme systems that are involved in different inflammatory pathologies, for example, in atherosclerosis. Moreover, it has been proposed that quercetin may reduce the risk of cardiovascular diseases by different mechanisms that include: i) the antioxidant activity that prevents LDL oxidation (Hayek et al., 1997; Osiecki, 2004); ii) inhibition of iNOS expression in inflammatory cells such as macrophages (Ortega et al., 2010); iii) reduction of platelet activity and aggregation (Pignatelli et al., 2000); iv) inhibition of vascular smooth muscle cells proliferation and migration (Alcocer et al., 2002); v) interference in the cardiovascular inflammation by inhibition of both the COX-2 and LOX-5 enzymes involved in the eicosanoid metabolism (Raso et al., 2001; Welton et al., 1988), and vi) the inhibition of the MMP-9 gene expression and protein secretion induced by TNF-α (a proinflammatory cytokine present in atherosclerotic lesions) in vascular smooth muscle cells (Moon et al., 2003). In all of these *in vitro* studies the concentration of quercetin that led to inhibition was relatively high (1–100 μM) (Kawai et al., 2008; Moon et al., 2003), and represented the same order of inhibitory concentration of MMP-9 proteolytic activity obtained in the present work (IC_{50} of ~20 μM). However, it is still unclear whether *in vitro* evidence can be extrapolated to an *in vivo* effect, and more work is necessary to investigate this possibility. Experimental evidence suggests that quercetin accumulates in the atherosclerotic lesions through the endothelial permeation of its major metabolite (quercetin-3-glucuronide) and subsequent deconjugation by intracellular and extracellular β-glucuronidase activity. (Kawai et al., 2008). Once in the intima vascular wall, quercetin may exert its atheroprotective activity by multiple molecular mechanisms, including the inhibition of active MMP-9 at the extracellular level. In this way, active MMP-9 represents one of the extracellular molecular targets for the cardioprotective action of quercetin, together with other molecular targets, including the intracellular signaling pathways involved in the induction of MMP-9 expression.

In conclusion, our data constitute the first evidence about possible interaction between quercetin and MMP-9, suggesting a mechanism to explain the inhibitory effect of the flavonoid against the proteolytic activity of the enzyme, which provides an additional molecular target for the cardioprotective activity of quercetin.

Acknowledgements

This work was supported in part by SECyT-UNC Nº 162/06 and Nº 69/08, FONCyT: BID 1728/OC-AR PICT N° 06-01207, 06-25667 and 07-01650, CONICET PIP 05-06 Nº 5421, SECyT-UBA 08-X625. A.C.S. is a doctoral fellow of SECyT-UNC, and M.G.O., J.L.C., D.A.E., M.A.M. and G.A.C. are members of the Research Career of CONICET. We are grateful to Dr. Paul David Hobson, native speaker, for revision of this manuscript.

Appendix A. Supplementary data

Supplementary data associated with this article can be found, in the online version, at doi:10.1016/j.ejphar.2010.07.001.

References

Alcocer, F., Whitley, D., Salazar-Gonzalez, J.F., Jordan, W.D., Sellers, M.T., Eckhoff, D.E., Suzuki, K., Macrae, C., Bland, K.I., 2002. Quercetin inhibits human vascular smooth muscle cell proliferation and migration. Surgery 131, 198–204.

Berendsen, H.J.C., Postma, J.P.M., Van Gunsteren, W.F., DiNola, A., Haak, J.R., 1984. Molecular dynamics with coupling to an external bath. J. Chem. Phys. 81, 3684–3690.

Bertini, I., Gupta, Y.K., Luchinat, C., Parigi, G., Peana, M., Sgheri, L., Yuan, J., 2007. Paramagnetism-based NMR restraints provide maximum allowed probabilities for the different conformations of partially independent protein domains. J. Am. Chem. Soc. 129, 12786–12794.

Bode, W., Maskos, K., 2003. Structural basis of the matrix metalloproteinases and their physiological inhibitors, the tissue inhibitors of metalloproteinases. Biol. Chem. 384, 863–872.

Bode, W., Fernandez-Catalan, C., Tschesche, H., Grams, F., Nagase, H., Maskos, K., 1999. Structural properties of matrix metalloproteinases. Cell. Mol. Life Sci. 55, 639–652.

Brambilla, D., Mancuso, C., Scuderi, M.R., Bosco, P., Cantarella, G., Lempereur, L., Di Benedetto, G., Pezzino, S., Bernardini, R., 2008. The role of antioxidant supplement in immune system, neoplastic, and neurodegenerative disorders: a point of view for an assessment of the risk/benefit profile. Nutr. J. 7, 29.

Cuccioloni, M., Mozzicafreddo, M., Bonfili, L., Cecarini, V., Eleuteri, A.M., Angeletti, M., 2009. Natural occurring polyphenols as template for drug design. Focus on serine proteases. Chem. Biol. Drug Des. 74, 1–15.

Cuniasse, P., Devel, L., Makaritis, A., Beau, F., Georgiadis, D., Matziari, M., Yiotakis, A., Dive, V., 2005. Future challenges facing the development of specific active-site-directed synthetic inhibitors of MMPs. Biochimie 87, 393–402.

Demeule, M., Brossard, M., Page, M., Gingras, D., Beliveau, R., 2000. Matrix metalloproteinase inhibition by green tea catechins. Biochim. Biophys. Acta 1478, 51–60.

Di Castelnuovo, A., Rotondo, S., Iacoviello, L., Donati, M.B., De Gaetano, G., 2002. Meta-analysis of wine and beer consumption in relation to vascular risk. Circulation 105, 2836–2844.

Diaz, N., Suarez, D., 2007. Molecular dynamics simulations of matrix metalloproteinase 2: role of the structural metal ions. Biochemistry 46, 8943–8952.

Erlund, I., Freese, R., Marniemi, J., Hakala, P., Alfthan, G., 2006. Bioavailability of quercetin from berries and the diet. Nutr. Cancer 54, 13–17.

Frisch, M.J., Trucks, G.W., Schlegel, H.B., Gill, P.M.W., Johnson, B.G., Robb, M.A., Cheeseman, J.R., Keith, T., Petersson, G.A., Montgomery, J.A., Raghavachari, K., Al-Laham, M.A., Zakrzewski, V.G., Ortiz, J.V., Foresman, J.B., Cioslowski, J., Stefanov, B.B., Nanayakkara, A., Challacombe, M., Peng, C.Y., Ayala, P.Y., Chen, W., Wong, M.W., Andres, J.L., Replogle, E.S., Gomperts, R., Martin, R.L., Fox, D.J., Binkley, J.S., Defrees, D.J., Baker, J., Stewart, J.P., Head-Gordon, M., Gonzalez, C., Pople, J.A., Gaussian, Inc., Pittsburgh PA, 1998.

Giovannini, C., Scazzocchio, B., Vari, R., Santangelo, C., D'Archivio, M., Masella, R., 2007. Apoptosis in cancer and atherosclerosis: polyphenol activities. Ann. Ist. Super. Sanità 43, 406–416.

Guglielmone, H.A., Agnese, A.M., Nunez Montoya, S.C., Cabrera, J.L., 2002. Anticoagulant effect and action mechanism of sulphated flavonoids from *Flaveria bidentis*. Thromb. Res. 105, 183–188.

Guglielmone, H.A., Agnese, A.M., Nunez Montoya, S.C., Cabrera, J.L., 2005. Inhibitory effects of sulphated flavonoids isolated from *Flaveria bidentis* on platelet aggregation. Thromb. Res. 115, 495–502.

Hayek, T., Fuhrman, B., Vaya, J., Rosenblat, M., Belinky, P., Coleman, R., Elis, A., Aviram, M., 1997. Reduced progression of atherosclerosis in apolipoprotein E-deficient mice following consumption of red wine, or its polyphenols quercetin or catechin, is associated with reduced susceptibility of LDL to oxidation and aggregation. Arterioscler. Thromb. Vasc. Biol. 17, 2744–2752.

Hornak, V., Abel, R., Okur, A., Strockbine, B., Roitberg, A., Simmerling, C., 2006. Comparison of multiple amber force fields and development of improved protein backbone parameters. Proteins: Struct. Funct. Genet. 65, 712–725.

Hu, X., Shelver, W.H., 2003. Docking studies of matrix metalloproteinase inhibitors: zinc parameter optimization to improve the binding free energy prediction. J. Mol. Graph. Model. 22, 115–126.

Humphrey, W., Dalke, A., Schulten, K., 1996. VMD: visual molecular dynamics. J. Mol. Graph. 14 (33–38), 27–38.
Huxley, R.R., Neil, H.A., 2003. The relation between dietary flavonol intake and coronary heart disease mortality: a meta-analysis of prospective cohort studies. Eur. J. Clin. Nutr. 57, 904–908.
Kawai, Y., Nishikawa, T., Shiba, Y., Saito, S., Murota, K., Shibata, N., Kobayashi, M., Kanayama, M., Uchida, K., Terao, J., 2008. Macrophage as a target of quercetin glucuronides in human atherosclerotic arteries: implication in the anti-atherosclerotic mechanism of dietary flavonoids. J. Biol. Chem. 283, 9424–9434.
Kiyama, R., Tamura, Y., Watanabe, F., Tsuzuki, H., Ohtani, M., Yodo, M., 1999. Homology modeling of gelatinase catalytic domains and docking simulations of novel sulfonamide inhibitors. J. Med. Chem. 42, 1723–1738.
Kleiner, D.E., Stetler-Stevenson, W.G., 1994. Quantitative zymography: detection of picogram quantities of gelatinases. Anal. Biochem. 218, 325–329.
Knekt, P., Jarvinen, R., Reunanen, A., Maatela, J., 1996. Flavonoid intake and coronary mortality in Finland: a cohort study. BMJ 312, 478–481.
Lang, R., Kocourek, A., Braun, M., Tschesche, H., Huber, R., Bode, W., Maskos, K., 2001. Substrate specificity determinants of human macrophage elastase (MMP-12) based on the 1.1 A crystal structure. J. Mol. Biol. 312, 731–742.
Lee, M.R., Duan, Y., Kollman, P.A., 2000. Use of MM-PB/SA in estimating the free energies of proteins: application to native, intermediates, and unfolded villin headpiece. Proteins 39, 309–316.
Li, Y.L., Xu, W.F., 2004. Design, synthesis, and activity of caffeoyl pyrrolidine derivatives as potential gelatinase inhibitors. Bioorg. Med. Chem. 12, 5171–5180.
Libby, P., 2002. Inflammation in atherosclerosis. Nature 420, 868–874.
Lu, Q., Luo, R., 2003. A Poisson–Boltzmann dynamics method with nonperiodic boundary condition. J. Chem. Phys. 119, 11035–11047.
Maron, D.J., 2004. Flavonoids for reduction of atherosclerotic risk. Curr. Atheroscler. Rep. 6, 73–78.
Matsuda, H., Morikawa, T., Toguchida, I., Yoshikawa, M., 2002. Structural requirements of flavonoids and related compounds for aldose reductase inhibitory activity. Chem. Pharm. Bull. (Tokyo) 50, 788–795.
Middleton Jr., E., Kandaswami, C., Theoharides, T.C., 2000. The effects of plant flavonoids on mammalian cells: implications for inflammation, heart disease, and cancer. Pharmacol. Rev. 52, 673–751.
Moon, S.K., Cho, G.O., Jung, S.Y., Gal, S.W., Kwon, T.K., Lee, Y.C., Madamanchi, N.R., Kim, C.H., 2003. Quercetin exerts multiple inhibitory effects on vascular smooth muscle cells: role of ERK1/2, cell-cycle regulation, and matrix metalloproteinase-9. Biochem. Biophys. Res. Commun. 301, 1069–1078.
Mukamal, K.J., Maclure, M., Muller, J.E., Sherwood, J.B., Mittleman, M.A., 2002. Tea consumption and mortality after acute myocardial infarction. Circulation 105, 2476–2481.
Newby, A.C., 2006. Matrix metalloproteinases regulate migration, proliferation, and death of vascular smooth muscle cells by degrading matrix and non-matrix substrates. Cardiovasc. Res. 69, 614–624.
Nguyen, M., Arkell, J., Jackson, C.J., 2001. Human endothelial gelatinases and angiogenesis. Int. J. Biochem. Cell Biol. 33, 960–970.
Ortega, M.G., Saragusti, A.C., Cabrera, J.L., Chiabrando, G.A., 2010. Quercetin tetraacetyl derivative inhibits LPS-induced nitric oxide synthase (iNOS) expression in J774A.1 cells. Archives of Biochemistry and Biophysics 498, 105–110.
Osiecki, H., 2004. The role of chronic inflammation in cardiovascular disease and its regulation by nutrients. Altern. Med. Rev. 9, 32–53.
Osterberg, F., Morris, G.M., Sanner, M.F., Olson, A.J., Goodsell, D.S., 2002. Automated docking to multiple target structures: incorporation of protein mobility and structural water heterogeneity in AutoDock. Proteins 46, 34–40.
Pasterkamp, G., Schoneveld, A.H., Hijnen, D.J., de Kleijn, D.P., Teepen, H., van der Wal, A.C., Borst, C., 2000. Atherosclerotic arterial remodeling and the localization of macrophages and matrix metalloproteases 1, 2 and 9 in the human coronary artery. Atherosclerosis 150, 245–253.
Pavlovsky, A.G., Williams, M.G., Ye, Q.Z., Ortwine, D.F., Purchase II, C.F., White, A.D., Dhanaraj, V., Roth, B.D., Johnson, L.L., Hupe, D., Humblet, C., Blundell, T.L., 1999. X-ray structure of human stromelysin catalytic domain complexed with nonpeptide inhibitors: implications for inhibitor selectivity. Protein Sci. 8, 1455–1462.
Pearlman, D.A., Case, D.A., Caldwell, J.W., Ross, W.S., Cheatham Iii, T.E., DeBolt, S., Ferguson, D., Seibel, G., Kollman, P., 1995. AMBER, a package of computer programs for applying molecular mechanics, normal mode analysis, molecular dynamics and free energy calculations to simulate the structural and energetic properties of molecules. Comput. Phys. Commun. 91, 1–41.
Peters, U., Poole, C., Arab, L., 2001. Does tea affect cardiovascular disease? A meta-analysis. Am. J. Epidemiol. 154, 495–503.
Pignatelli, P., Pulcinelli, F.M., Celestini, A., Lenti, L., Ghiselli, A., Gazzaniga, P.P., Violi, F., 2000. The flavonoids quercetin and catechin synergistically inhibit platelet function by antagonizing the intracellular production of hydrogen peroxide. Am. J. Clin. Nutr. 72, 1150–1155.
Pirard, B., Matter, H., 2006. Matrix metalloproteinase target family landscape: a chemometrical approach to ligand selectivity based on protein binding site analysis. J. Med. Chem. 49, 51–69.
Rahat, M.A., Marom, B., Bitterman, H., Weiss-Cerem, L., Kinarty, A., Lahat, N., 2006. Hypoxia reduces the output of matrix metalloproteinase-9 (MMP-9) in monocytes by inhibiting its secretion and elevating membranal association. J. Leukoc. Biol. 79, 706–718.
Rao, B.G., 2005. Recent developments in the design of specific matrix metalloproteinase inhibitors aided by structural and computational studies. Curr. Pharm. Des. 11, 295–322.
Raso, G.M., Meli, R., Di Carlo, G., Pacilio, M., Di Carlo, R., 2001. Inhibition of inducible nitric oxide synthase and cyclooxygenase-2 expression by flavonoids in macrophage J774A.1. Life Sci. 68, 921–931.
Rice-Evans, C.A., Miller, N.J., Paganga, G., 1996. Structure–antioxidant activity relationships of flavonoids and phenolic acids. Free Radic. Biol. Med. 20, 933–956.
Rowsell, S., Hawtin, P., Minshull, C.A., Jepson, H., Brockbank, S.M., Barratt, D.G., Slater, A.M., McPheat, W.L., Waterson, D., Henney, A.M., Pauptit, R.A., 2002. Crystal structure of human MMP9 in complex with a reverse hydroxamate inhibitor. J. Mol. Biol. 319, 173–181.
Ryckaert, J.P., Ciccotti, G., Berendsen, H.J.C., 1977. Numerical integration of the Cartesian equations of motion of a system with constraints: molecular dynamics of n-alkanes. J. Comput. Phys. 23, 327–341.
Sartor, L., Pezzato, E., Dell'Aica, I., Caniato, R., Biggin, S., Garbisa, S., 2002. Inhibition of matrix-proteases by polyphenols: chemical insights for anti-inflammatory and anti-invasion drug design. Biochem. Pharmacol. 64, 229–237.
Silva, M.M., Santos, M.R., Caroco, G., Rocha, R., Justino, G., Mira, L., 2002. Structure–antioxidant activity relationships of flavonoids: a re-examination. Free Radic. Res. 36, 1219–1227.
Stawowy, P., Meyborg, H., Stibenz, D., Borges Pereira Stawowy, N., Roser, M., Thanabalasingam, U., Veinot, J.P., Chretien, M., Seidah, N.G., Fleck, E., Graf, K., 2005. Furin-like proprotein convertases are central regulators of the membrane type matrix metalloproteinase-pro-matrix metalloproteinase-2 proteolytic cascade in atherosclerosis. Circulation 111, 2820–2827.
Tuccinardi, T., Martinelli, A., Nuti, E., Carelli, P., Balzano, F., Uccello-Barretta, G., Murphy, G., Rossello, A., 2006. Amber force field implementation, molecular modelling study, synthesis and MMP-1/MMP-2 inhibition profile of (R)- and (S)-N-hydroxy-2-(N-isopropoxybiphenyl-4-ylsulfonamido)-3-methylbutanamides. Bioorg. Med. Chem. 14, 4260–4276.
van't Veer, P., Jansen, M.C., Klerk, M., Kok, F.J., 2000. Fruits and vegetables in the prevention of cancer and cardiovascular disease. Public Health Nutr. 3, 103–107.
Walker, E.H., Pacold, M.E., Perisic, O., Stephens, L., Hawkins, P.T., Wymann, M.P., Williams, R.L., 2000. Structural determinants of phosphoinositide 3-kinase inhibition by wortmannin, LY294002, quercetin, myricetin, and staurosporine. Mol. Cell 6, 909–919.
Wang, J., Cieplak, P., Kollman, P.A., 2000. How well does a restrained electrostatic potential (RESP) model perform in calculating conformational energies of organic and biological molecules? J. Comput. Chem. 21, 1049–1074.
Wang, J., Wolf, R.M., Caldwell, J.W., Kollman, P.A., Case, D.A., 2004. Development and testing of a general amber force field. J. Comput. Chem. 25, 1157–1174.
Welton, A.F., Hurley, J., Will, P., 1988. Flavonoids and arachidonic acid metabolism. Prog. Clin. Biol. Res. 280, 301–312.
Zhang, S., Yang, X., Coburn, R.A., Morris, M.E., 2005. Structure activity relationships and quantitative structure activity relationships for the flavonoid-mediated inhibition of breast cancer resistance protein. Biochem. Pharmacol. 70, 627–639.